Estuaries and Coasts
https://doi.org/10.1007/s12237-020-00757-6

Oxygen and Triple Oxygen Isotope Measurements Provide Different Insights into Gross Oxygen Production in a Shallow Salt Marsh Pond

Evan M. Howard[1] · Amanda C. Spivak[2] · Jennifer S. Karolewski[3] · Kelsey M. Gosselin[4] · Zoe O. Sandwith[5] · Cara C. Manning[6] · Rachel H. R. Stanley[7]

Received: 10 January 2020 / Revised: 5 May 2020 / Accepted: 8 May 2020

Abstract

The metabolism of estuarine environments is often estimated by measuring changes in dissolved oxygen concentrations. A central assumption of common oxygen-based approaches is that oxygen consumption rates (primarily respiration) are similar under light and dark conditions. Evaluating this assumption is critical, especially in benthic-dominated systems, because differences between daytime and nighttime respiration could result in underestimation or overestimation of ecosystem productivity. We evaluated rates of gross oxygen production over hourly to seasonal time scales in a shallow, temperate salt marsh pond. To assess whether a dissolved oxygen diel mass balance underestimated gross oxygen productivity, we compared rates using this traditional approach and using the triple oxygen isotope tracer of photosynthesis. This is a powerful combination because the triple oxygen isotope approach is theoretically insensitive to respiration. The methods agreed well over daily to seasonal time scales. However, during midday periods of peak light and productivity, the triple oxygen isotope approach resulted in higher hourly scale gross oxygen production rates. The timing and magnitude of this short-term difference is consistent with light-dependent oxygen uptake fluxes including photoreduction and/or light-stimulated community respiration. Finally, aquatic vegetation was associated with variability in productivity across the pond. Such small-scale environmental heterogeneity is evidence that this shallow pond was not laterally well mixed, and likely contributes to the dynamism of these common estuarine environments.

Keywords Metabolism · Light-dependent respiration · Oxygen · Triple oxygen isotopes · Salt marsh · Pond

Introduction

Dissolved oxygen (O_2) fluxes are widely used to estimate aquatic ecosystem metabolism rates, including in lakes (Staehr et al. 2010), streams (Demars et al. 2015), estuaries (Caffrey 2004), and the ocean (Yang et al. 2017). However, attribution of these fluxes to photosynthesis and respiration is complicated because the physical and biological processes that affect net oxygen fluxes vary over time and space and may be difficult to disentangle without additional tracers. In

Communicated by Isaac Santos

Electronic supplementary material The online version of this article (https://doi.org/10.1007/s12237-020-00757-6) contains supplementary material, which is available to authorized users.

✉ Evan M. Howard
ehoward2@uw.edu

[1] School of Oceanography, University of Washington, Seattle, WA, USA

[2] Department of Marine Sciences, University of Georgia, Athens, GA, USA

[3] MIT-WHOI Joint Program in Oceanography, Cambridge and Woods Hole, MA, USA

[4] Department of Earth Science, University of California Santa Barbara, Santa Barbara, CA, USA

[5] Department of Marine Chemistry and Geochemistry, Woods Hole Oceanographic Institution, Woods Hole, MA, USA

[6] Department of Earth, Ocean and Atmospheric Sciences, University of British Columbia, Vancouver, BC, Canada

[7] Department of Chemistry, Wellesley College, Wellesley, MA, USA

Published online: 18 July 2020

particular, deriving photosynthesis rates from a dissolved O_2 mass balance typically requires either assuming that nighttime respiration is representative of daytime respiration (e.g., Odum 1956; Staehr et al. 2010) or using submodels of photosynthesis as a function of irradiance and respiration as a function of temperature (Holtgrieve et al. 2010; Winslow et al. 2016). Neither approach accounts for light-dependent increases in ecosystem respiration or non-respiratory O_2 uptake. Yet, O_2 consumption in aquatic ecosystems including sediments and pelagic environments in lakes, estuaries, and the open ocean may be two to ten times greater in the light than in the dark (Falkowski and Owens 1978; Bender et al. 1987; Kana 1990; Epping and Jørgensen 1996; Parkhill and Gulliver 1998; Pringault et al. 2009). The same studies found that if light-dependent O_2 uptake is not explicitly accounted for, photosynthetic production may be underestimated by 23–62%.

Thus, ecosystem rates of photosynthesis and respiration based on dissolved O_2 fluxes may be systematically too low, complicating assessment of O_2-driven biogeochemistry and attribution of changes in ecosystem metabolism rates to environmental drivers.

Observations of light-dependent O_2 consumption are generally derived from concurrent comparisons between net O_2 fluxes and either production or respiration, separately evaluated using other methods. Some studies measure either short-term responses to light, including methods based on fluorometry (Suggett et al. 2009) and hysteresis of dissolved O_2 responses to irradiance changes (Falkowski and Owens 1978; Epping and Jørgensen 1996). Others compare net O_2 or carbon fluxes to photosynthetic production evaluated with carbon or oxygen isotope labeling of photosynthetic substrates (Bender et al. 1987; Laws et al. 2000). Laboratory studies may inhibit specific cellular pathways in order to isolate the particular light-dependent O_2 process of interest (e.g., Helman et al. 2005). Each method has different sensitivities to different mechanisms of O_2 uptake. This diversity of tracers and methods used can complicate the attribution of measured O_2 fluxes to specific light-dependent processes as opposed to methodological biases. It is therefore challenging to generalize the wide range of light-dependent effects on respiration and productivity reported in the literature.

One promising approach for estimating in situ photosynthesis in aquatic environments is the triple oxygen isotope (TOI) method (Luz and Barkan 2000), which involves the simultaneous measurement of natural abundance ^{16}O, ^{17}O, and ^{18}O of O_2 dissolved in water. The oxygen isotope ratios can be combined in a respiration-independent manner in order to calculate the fraction of dissolved O_2 derived from splitting of water in photosystem II during photosynthesis compared to the fraction of O_2 entering the water through air-water gas exchange. Thus the evolution of the oxygen isotope ratios with time provides an unambiguous estimate of gross oxygen production (GOP), similar to the $H_2{}^{18}O$ isotopic spike method (Bender et al. 1987). However, a crucial difference between the TOI method and $H_2{}^{18}O$ or other incubation methods is that the natural abundance triple oxygen isotopes can be used to evaluate photosynthesis in situ, in intact ecosystems, whereas incubation methods require removing organisms from their natural system (e.g., into bottles). Used in this way, the TOI method for estimating GOP shares a major source of systematic uncertainty with the dissolved O_2-derived production: air-water gas exchange. This facilitates a direct comparison with dissolved O_2 fluxes derived from in situ sensors in a common O_2 "currency," and allows evaluation of O_2 uptake in the light under ambient environmental conditions. The shared uncertainties and sensitivity to in situ conditions of these two methods contrasts with the primarily incubation-based approaches outlined above, in which results may diverge from whole ecosystem production and respiration rates because of altered growth environments ("bottle effects") or subsampling of the heterogeneous autotrophic and heterotrophic community of organisms.

Differences between TOI and dissolved O_2-derived rates of gross O_2 production should directly reflect the importance of light-dependent O_2 uptake processes (see "Light-Dependent Oxygen Uptake Processes" section). Yet, despite this potential utility and increasing adoption of this approach (e.g., Juranek and Quay 2013), the TOI method has rarely been directly compared to GOP from dissolved O_2 fluxes. Sarma et al. (2005) reported GOP from in situ TOI measurements to be nearly twice that derived from O_2 in light-dark bottle incubations for the surface mixed-layer of a coastal setting, though that ratio varied seasonally. In a Lagrangian study in the surface mixed layer of the pelagic ocean, Hamme et al. (2012) found that in situ GOP rates from the TOI method ranged from half to double the GOP from an O_2 diel mass balance, though the two rates were not significantly different after a sufficiently long period elapsed. In a shallow estuary, Stanley and Howard (2013) found that the GOP derived from either method agreed when both the oxygen isotopes and dissolved O_2 were measured in benthic chambers at hourly frequencies. To the best of our knowledge, no previously published work has compared in situ GOP fluxes from the two methods across the range of time scales (hourly to seasonal) that O_2 data are commonly collected for studies of freshwater and estuarine metabolism.

In this work, we compare in situ photosynthetic rates derived from a standard dissolved O_2 diel mass balance to those from the TOI method in a salt marsh pond. These shallow, continuously submerged environments are well-lit, highly productive, have high rates of aerobic and anaerobic sedimentary respiration producing reduced compounds, and undergo large diel changes in O_2 concentrations (Spivak et al. 2017, 2018). These characteristics have been identified as likely to stimulate light-dependent O_2 uptake in other environments (Falkowski and Raven 1997; Fenchel and Glud 2000;

Buapet et al. 2013). Because we apply both the TOI and dissolved O_2 mass balance methods to in situ data collected at the same time from the same salt marsh pond, sources of systematic error between approaches are limited and incubation effects are eliminated; any differences in O_2 production rates between the two approaches are more confidently assigned to light-dependent O_2 uptake. Our goals are to: (1) evaluate whether GOP rates from the TOI and dissolved O_2 diel mass balance are in good agreement or show systematic biases over seasonal, daily, or hourly time scales; (2) determine the magnitude and significance of light-dependent O_2 uptake in this setting; and (3) discuss the relationship of TOI and dissolved O_2-derived ecosystem metabolism fluxes to variations in environmental properties.

Methods

Theory

Dissolved O_2 Diel Method

The dissolved oxygen mass balance for a parcel of water depends on production, respiration, air-water gas exchange, light-dependent processes that consume O_2, entrainment and mixing with adjacent water parcels, and bubble processes including wave driven bubble injection and partial bubble exchange, and ebullition from underlying sediments. We do not quantify mixing or bubble processes, as neither could be adequately constrained over the entire study period, but consider the effects of these processes in the discussion. The resulting simplified O_2 mass balance for a well-mixed water parcel is expressed as:

$$h\frac{\partial}{\partial t}([O_2]) = GOP_{O2} - R + k_{O2}\left([O_2]_{sat} - [O_2]\right) - LD \qquad (1)$$

Here, h is the depth of the well-mixed water parcel being considered, $[O_2]$ and $[O_2]_{sat}$ are the measured and air-water saturation (at equilibrium) concentrations of dissolved O_2, GOP_{O2} is the areal gross oxygen production rate, R is the areal community respiration rate, k_{O2} is the air-water gas transfer velocity, and LD is the areal rate of a light-dependent process that results in net consumption of O_2. k_{O2} is calculated from wind speed and pond area using the parameterization of Vachon and Prairie (2013).

Only the sum of the oxygen-producing and oxygen-consuming processes can be directly evaluated from dissolved O_2 data. If light-dependent processes are minor contributors then the net biological O_2 flux is equivalent to net ecosystem metabolism (NEM = $GOP_{O2} - R$, sometimes alternatively referred to as net community production). In order to calculate GOP_{O2}, R is assumed to equal net oxygen uptake measured during nighttime periods (GOP_{O2} and PD equal zero) and further assumed to be identical in the day (Odum 1956). We use this simple approach and note that it yields similar results to more nuanced calculations (Spivak et al. 2017) informed by temperature dependence of respiration and production (Yvon-Durocher et al. 2012) and light-dependent parameterizations of photosynthesis (Winslow et al. 2016). To the degree this assumption is incorrect, GOP_{O2} and GOP derived from the triple oxygen isotopes (GOP_{TOI}) would diverge in a manner which provides additional information about environmental drivers of respiration.

Triple Oxygen Isotope Method

Ratios of the three stable oxygen isotope ratios ($^{18}O/^{17}O/^{16}O$) can be used to define the TOI tracer $^{17}\Delta$ (defined after Angert et al. 2003):

$$^{17}\Delta = \left[\ln\left(^{17}X\right) - \lambda\ln\left(^{18}X\right)\right] \times 10^6 \text{per meg} \qquad (2)$$

^{i}X relates the isotopic ratio of dissolved oxygen (i denotes the heavier isotope) to that in the atmospheric air standard, e.g., $^{i}X = (^{i}O/^{16}O)_{sample} / (^{i}O/^{16}O)_{air}$. Per meg notation is used to denote part per million level variation in gas ratios (Keeling et al. 1998). λ is the ratio of the mass-dependent isotope enrichment factors for $^{17}O/^{16}O$ and $^{18}O/^{16}O$. λ is constant within uncertainties for mitochondrial respiration (and photorespiration via RuBisCo) in the photosynthesizers cultured and measured to date ($\lambda = 0.518$; Helman et al. 2005; Luz and Barkan 2005; Eisenstadt et al. 2010); thus, $^{17}\Delta$ is defined to be respiration independent with λ. We use this conventional value to represent the pond community, however, recent work suggests that a higher value ($\lambda = 0.522$) is better supported by theory and recent dark respiration experiments in a freshwater reservoir (Ash et al. 2020); substituting this higher value results in qualitatively similar results in this work and does not alter our conclusions (ESM S1).

Photosynthetic O_2 has a high value of $^{17}\Delta$ similar to the isotopic composition of the water from which it is derived (Luz and Barkan 2000), while atmospheric oxygen has low $^{17}\Delta$ resulting from mass-independent fractionation of ozone in the stratosphere (Thiemens 2001). Therefore, greater values of $^{17}\Delta$ in dissolved O_2 indicate increased photosynthetic production relative to gas exchange with the atmosphere.

Gross primary production-independent of normal, mitochondrial respiration can then be calculated from an isotopic mass balance of dissolved oxygen (Kaiser 2011; Prokopenko et al. 2011). We provide full derivations and equations for the triple oxygen isotopic mass balance in ESM S2, including mixing and bubble processes not quantified in this work. The resulting abbreviated isotopic mass balance in terms of the measured isotopic ratios and $^{17}\Delta$:

$$h[O_2]\frac{\partial}{\partial t}\left({}^{17}\Delta\right) \quad \text{Change in tracer with time} \tag{3a}$$

$$= \mathrm{GOP_{TOI}}\left(\frac{{}^{17}X_w\,{}^{17}\alpha_p - {}^{17}X}{{}^{17}X} - \lambda\frac{{}^{18}X_w\,{}^{18}\alpha_p - {}^{18}X}{{}^{18}X}\right) \quad \text{Gross oxygen production} \tag{3b}$$

$$+k_{O2}[O_2]_{sat}\left(\frac{{}^{17}X_a\,{}^{17}\alpha_e\,{}^{17}\alpha_k - {}^{17}X}{{}^{17}X} - \lambda\frac{{}^{18}X_w\,{}^{18}\alpha_e\,{}^{18}\alpha_k - {}^{18}X}{{}^{18}X}\right) \quad \text{Air–water gas exchange}$$
$$-k_{O2}[O_2]\left(\left({}^{17}\alpha_k - 1\right) - \lambda\left({}^{18}\alpha_k - 1\right)\right) \tag{3c}$$

$$-\mathrm{LD}\left(\left({}^{17}\alpha_{ld} - 1\right) - \lambda\left({}^{18}\alpha_{ld} - 1\right)\right) \quad \text{Light–dependent process} \tag{3d}$$

X_a and X_w refer to the isotopic endmembers for air (1 when air is the reference) and water (calculated as a mixture of seawater and meteoric water; Manning et al. 2017). X without a subscript refers to the measured ratios of dissolved O_2. α represents the isotopic fractionation factors associated with production (α_p, kinetic; Eisenstadt et al. 2010; Luz and Barkan 2011), air-water gas exchange (α_e, equilibrium; Benson and Krause Jr. 1980, 1984; Reuer et al. 2007; α_k, kinetic; Li et al. 2019), and the light-dependent process of interest (α_{pd}, kinetic; Helman et al. 2005)—Eq. 3d assumes that the light-dependent process removes O_2 isotopically similar to that in the surrounding water rather than directly consuming O_2 from photosystem II (Kana 1990; Bender et al. 1999). Constants are chosen or calculated based on the preceding references (and summarized in ESM S2); however, other choices may be appropriate for alternative definitions of ${}^{17}\Delta$ (Kaiser 2011; Nicholson 2011; Kaiser and Abe 2012). The rate of bulk O_2 change is explicitly included in the derivation of Eqs. 3a–3d (Kaiser 2011; Prokopenko et al. 2011). ESM S2 includes an example calculation. The MATLAB toolbox "calcGOP" also may be used to calculate resulting $\mathrm{GOP_{TOI}}$ using Eqs. 3a–3c (with the simplifying assumptions that $\alpha_k = 1$ and α_p is the average value for marine phytoplankton; Manning and Howard 2017).

Light-Dependent Oxygen Uptake Processes

Light-dependent O_2 consumption is variously attributed to five major processes: photoreduction (Falkowski and Raven 1997), photorespiration (Buapet et al. 2013), light stimulation of mitochondrial ("dark") respiration in autotrophs (Grande et al. 1989), indirect stimulation of heterotroph respiration via release of labile dissolved organic carbon by photosynthesizers (Laws et al. 2000; Pringault et al. 2009), and, in benthic environments, oxidation of reduced compounds stored in sediments (Fenchel and Glud 2000). Each of these processes are expected to lead to larger $\mathrm{GOP_{TOI}}$ than $\mathrm{GOP_{O2}}$: Photoreduction can cause higher $\mathrm{GOP_{TOI}}$ but does not affect $\mathrm{GOP_{O2}}$, while the other processes all decrease $\mathrm{GOP_{O2}}$ but are not expected to significantly affect $\mathrm{GOP_{TOI}}$. These effects are summarized in Table 1 and described further in ESM S1.

Data Collection and Analysis

Setting

The study site was a salt marsh pond, located at the Plum Island Ecosystems Long-Term Ecological Research site in Massachusetts, USA (42.7411° N, 70.8309° W). The pond was approximately 7000 m^2 in area with a 25 cm mean depth. The pond was situated in the high marsh, which is predominantly vegetated by *Spartina patens*, and proximal to a tidal creek. The pond flooded with water from the surrounding tidal creek during the highest spring tides, roughly once daily over a few successive days every two weeks. Ecosystem metabolism and environmental heterogeneity (Spivak et al. 2017, 2018), diel cycling of microbial processes (Kearns et al. 2017), and air-water gas exchange and ebullition (Howard et al. 2018) have been previously examined in this pond.

Sampling Methods

Temperature, electrical conductivity (and resulting salinity), and O_2 saturation data were collected at 15 min frequency from May 7 to 28 October 2014. Sensor data were recorded at a single location over sediment without macrophytes, far from the pond banks (Fig. 1). Sensors were deployed approximately 10 cm above the sediment-water interface. The sensors were cleaned and calibrated (pre- and post-deployment) approximately every 2 weeks. Calibrations included 1-point O_2 calibration to water-saturated air (with initial zero-O_2 calibration in May 2014), and 2-point conductivity calibrations (1×10^4 and 5×10^4 μS cm^{-1} YSI standards). Additional details of sensor deployment, cross-calibration, and post hoc correction of salinity are in the supporting information (ESM S2)—no sensor drift or offsets between different sensor deployments were observed for temperature and O_2.

Photosynthetically active radiation flux (PAR, 400–700 nm wavelengths) and meteorological data used to calculate air-water gas exchange were collected at a meteorological tower 200 m northeast from the study site (Forbrich and Giblin 2015). Air-water gas exchange was calculated from meteorological data as described in Howard et al. (2018) using the wind speed based parameterization of Vachon and Prairie (2013). In situ and air-water equilibrium concentrations of O_2, $[O_2]$, and $[O_2]_{eq}$ (Garcia and Gordon 1992, 1993) were smoothed using a 30 min ($n = 3$) moving mean to limit instrument signal noise.

Samples for TOI analysis were collected approximately weekly, during 20 daytime periods when the pond was tidally isolated from the adjacent tidal creek. Pond water was collected in pre-poisoned, 500 mL evacuated glass flasks, which were filled with roughly 300 mL of water while submerged at 10 cm depth. Care was taken to exclude bubbles and debris, and samples were collected 2 m from the pond edge using an

Table 1 Sources of light-dependent divergence in gross oxygen production

Process	Effect on GOP		Greatest daytime difference
	GOP_{O2}	GOP_{TOI}	
Photoreduction	No change	Overestimate	Midday, at high light
Photorespiration	Underestimate	No change	In afternoon, when partial pressures of O_2 are highest and CO_2 lowest
Light-stimulated autotrophic respiration	Underestimate	No change	Midday, at high productivity
Indirect stimulation of heterotrophic respiration	Underestimate	No change	Midday, at high productivity
Oxidation of sediment compounds	Underestimate	No change or underestimate[a]	In morning, after overnight accumulation of sediment oxygen debt

Light-dependent oxygen update processes that could lead to divergence in gross oxygen production derived from the diel-dissolved oxygen mass balance and the triple oxygen isotope method (GOP_{O2} and GOP_{TOI}). Also, the time of day the two GOP rates are expected to diverge most if a particular process leads to observable differences. These processes are discussed in greater detail in ESM S1

[a] Dissolved oxygen that is completely produced and consumed within the sediments will not influence the isotopic characteristics of the bulk O_2 pool measured in the water column, which could cause both GOP rates to underestimate daytime productivity and diverge by less. See ESM S1

inner-tube to avoid suspending sediments during sampling. Samples were collected over bare sediments at three or more timepoints between 10:00 and 14:00, with a few days

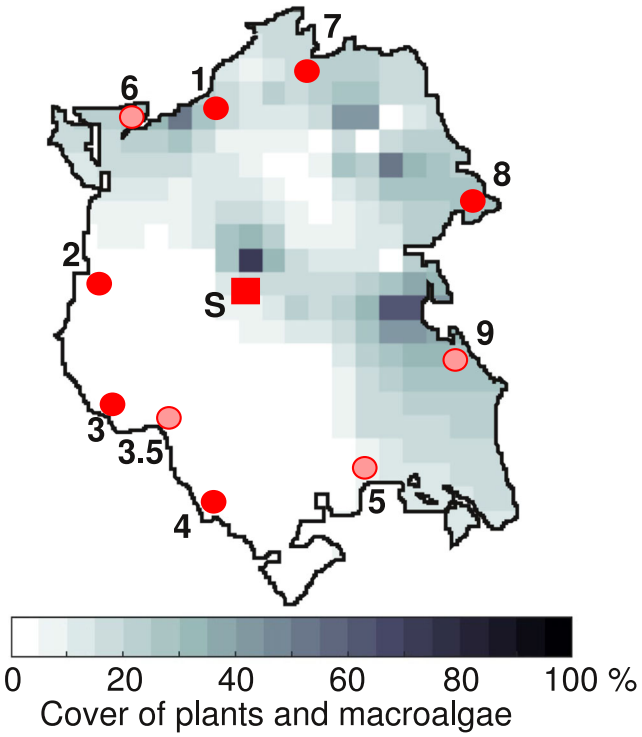

Fig. 1 (color figure online) Map of sensor (S, red square) and sample locations (numbers, red circles). North is top of figure. Light red circles indicate locations where a subset of tracers were sampled, but GOP_{TOI} was not evaluated. Gray shading and colorbar indicates vegetation cover, averaged over the seasonal sampling period, and interpolated or extrapolated over a 5×5 m^2 resolution grid (see text). Sensor was located over unvegetated sediment, but was within 2–3 m of vegetation cover. The southernmost portion of the pond near sample location 4 had some vegetation but was not quantitatively surveyed

including early morning and evening periods. Additionally, concurrent time series over macroalgae (*Ulva intestinalis*) or rooted vascular plants (*Ruppia maritima*) were collected on several days. In order to evaluate replicate uncertainty in the TOI samples, two to five replicate samples were collected at 19 different times over the course of the study.

Additional O_2 saturation state, temperature, and salinity data were collected simultaneously with each TOI bottle sample using a handheld YSI Pro-ODO sensor (accuracy and precision 0.1 ± 0.2 °C and 2 ± 0.2 % of oxygen saturation) and handheld refractometer (2± on PSS-78). Both instruments were calibrated daily. Along the western edge of the pond where most daily time series were conducted, these measurements were similar to conditions at the sensor location. However, conditions were more varied around the pond perimeter, particularly on the eastern side of the pond where submerged grasses and macroalgae were more abundant. O_2 saturation state and temperature were surveyed in the morning and midday on May 29th, July 17th, July 23rd; August 7th, September 23rd, and October 13th.

Total sediment cover of submerged *Ruppia* and *Ulva* was visually estimated over 11 weeks between June 25th and August 13th, as well as between 11th and November 25th (Spivak et al. 2017). On each occasion, macrophyte cover was assessed from three 1 m^2 quadrats randomly sampled along each of two crossing transects (different transects for each sample period) for a total of six sample locations. All percent cover data were pooled to map the average conditions over the sampling season and binned and averaged over a 5×5 m grid. To fill missing data, we used an image interpolation and extrapolation approach (MATLAB function "inpaint_nans," method 4; D'Errico 2012). This method generates equivalent results to linear interpolation, but behaves conservatively during spatial extrapolation to fill missing data

within the limits of (no higher than) adjacent sampled data (ESM S1).

Triple Oxygen Isotope Analysis

Water and gas headspace in the TOI samples were equilibrated at room temperature, and the headspace was processed on an automated cryogenic line which collected O_2 and Argon (Ar) while separating and discarding water vapor and dinitrogen gas (Stanley and Howard 2013). Oxygen isotope ratios were measured on a Thermo Scientific MAT 253 isotope ratio mass spectrometer. Every sample was compared to a gas secondary standard with similar O_2/Ar to seawater (Scott Specialty Gases); sample and standard voltages were balanced, resulting in similar pressure within the mass spectrometer. Samples were additionally referenced to both a gas primary standard (atmospheric air from Woods Hole, MA, USA) and air-equilibrated de-ionized water (blank solutions with no biological signature), which were run every nine samples. Samples were corrected for ion source interactions with Ar (Abe and Yoshida 2003) when O_2/Ar ratios were sufficiently high that Ar matrix corrections were less than roughly 10% of the magnitude of measured isotope ratios, which was generally true at >70% of O_2 saturation. At lower O_2/Ar ratios (e.g., early morning samples), Ar and any trace methane was additionally stripped from the gas sample prior to measurement (ESM S1). Using either method, the oxygen isotope ratios were additionally corrected for sample size (Stanley et al. 2010) and small differences between $^{17}\Delta$ calculated from calibrated $^{18}O/^{16}O$ and $^{17}O/^{16}O$ versus those on $^{17}\Delta$ directly (Howard 2017) in order to determine precise isotope ratios over the entire range of O_2 concentrations in the pond. Each calibration was well described as a linear function of isotopic composition (a few percent relative error in the slopes). There was no indication that pressure baseline errors were an important source of uncertainty following calibrations, in either the O_2/Ar or pure O_2 samples (ESM S1).

Water standards run concurrently with our samples were precise to 3×10^{-2} per mil in $^{17}O/^{16}O$, 5×10^{-2} per mil in $^{18}O/^{16}O$, and 6 per meg in $^{17}\Delta$ (6×10^{-3} per mil; standard deviations for $n = 51$ water standards). Sample replicate precision was 7×10^{-2} per mil in $^{17}O/^{16}O$, 13×10^{-2} per mil in $^{18}O/^{16}O$, and 5 per meg in $^{17}\Delta$ (4% relative error in all three measures). Water standards were not significantly different using either the high or low O_2/Ar ratio methods ($p > 0.9$ for Welch's t-test with null hypothesis of different population means for all isotopic variables).

Ecosystem Metabolism Rate Calculations

Equations 1 and 3 were discretized and rearranged to determine particular rates of interest. Changes over the period spanning two sampled times were calculated using midpoint values of the continuous variables (e.g., concentrations, air-water gas transfer velocity, isotopic ratios). For direct comparison of hourly GOP_{TOI} and GOP_{O2}, GOP_{O2} was averaged over a 90 min window centered on the time of GOP_{TOI}, similar to the TOI sampling frequency.

In order to compare full day rates of GOP_{TOI} and GOP_{O2}, integrated GOP_{TOI} during the midday observational period was multiplied by the ratio of the integrated dawn-dusk PAR over the integrated PAR during the TOI sampling period. We took this simple scaling approach because a single photosynthesis-irradiance (P-I) curve could not fit all the GOP results over the six month time series, and there were generally insufficient data to fit daily P-I curves. However, unsampled periods were generally at low PAR, where GOP and PAR should have been linearly related. Indeed, even without excluding samples from periods likely beyond the saturating irradiance, integrated GOP_{TOI} and PAR over each hour-scale measurement period were significantly linearly correlated ($r = 0.53$, $p = 3\times10^{-7}$ for a null hypothesis of no correlation, 35% uncertainty in correlation slope). Further, the unsampled morning and evening periods generally contributed less than a quarter of integrated PAR. Thus the theoretical errors associated with this approach ($\leq$ 20%, relative standard deviation) were of similar size to other uncertainties. For the three daily time series in which TOI was sampled in mornings and evenings, daily GOP_{TOI} agreed well with the PAR-scaled daily GOP_{TOI} derived from the 10:00–14:00 samples—the ratio of measured to scaled GOP_{TOI} was 1.0(0.1; standard deviation; no bias between rates).

Both hourly and daily average rates are reported in terms of areal production per hour, for comparability of the magnitude and variability of rates over different time scales.

Statistics

In order to examine environmental variability, the effect of the variability of O_2 changes was calculated by taking the standard deviation of all measured rates of change at each sample location over the study and dividing by the average of standard deviations at all sample locations. This normalized effect size highlights where in the pond temporal variability in oxygen changes is highest or lowest—e.g., an effect size of 2 means that on average, O_2 saturation state at a location increased twice as much as the mean across the pond.

GOP, R, and NEM errors were propagated from each input variable's standard probability distribution via a Monte Carlo simulation with 10,000 iterations, with the standard deviation across all iterations reported as the rates' uncertainties. Shared sources of systematic uncertainty between both TOI and dissolved O_2-derived metabolic rates were not included in uncertainty estimates (e.g., uncertainties in the parameterizations of the gas transfer velocity and O_2 solubility), but random errors expected to vary between sample locations and times were included (e.g., short-term variability in wind, instrumental precision of measured O_2 saturation state, and changes in solubility driven by temperature heterogeneity within the pond).

Uncertainties for subsequent comparisons of metabolic rates were calculated in quadrature.

In order to determine whether short, daily to weekly changes of environmental parameters in time contributed to changes in daily GOP_{O2} and R, the time series of each environmental property considered (temperature, PAR, windspeed, wind direction, and tidal flooding) were detrended to remove autocorrelation (prewhitened) using an Autoregressive Integrated Moving Average (ARIMA) procedure with the "arima.m" function in MATLAB. Differencing, autoregressive (lag), and moving average (smoothing) terms were assigned based on analysis of the autocorrelation and partial autocorrelation functions of for the variables of interest, with the goal of reducing the residuals of the observations versus the ARIMA model to white noise. An additional periodic term was used in the tidal stage ARIMA. The cross-correlation coefficients (r) between the residuals of the environmental variable and metabolic rates relative to the ARIMA model for that environmental variable were then calculated.

Correlations of GOP_{TOI} with environmental variables were calculated based on only the subset of data from days when GOP_{TOI} was sampled. Data were not prewhitened for any variables in this reduced subset because of the small number of samples and discontinuous time series—autocorrelations and partial-autocorrelations were already near zero and not reduced by an ARIMA procedure.

Throughout, p values are presented for the following statistical tests, unless otherwise specified: Significance of linear correlations are evaluated for the null hypotheses of no correlation or a regression differing in sign (a one-tailed distribution), using Fisher's z-transformation on the linear correlation coefficients, r, and evaluating resulting tails of the normal cumulative distribution functions. Alternatively, significance of bias (mean rate difference of one method relative to the other) is evaluated with the null hypothesis of zero difference using a paired sample Student's t-test. Standard deviations or relative standard deviations are noted in parentheses following mean values (e.g., mean (standard deviation)). Linear correlations use Model II regressions, in which root mean square errors are calculated normal to the regression slope (neither variable is assumed to be independent and error free); r are reported for the linearity of regressions, and, where data is normally distributed, r^2 is used to calculate the fraction of total variance shared by regressed variables.

Results

Metabolic Rate Comparison

On hourly time scales, GOP_{O2} and GOP_{TOI} (Fig. 2a–c) were significantly correlated ($r = 0.45$, $p = 1\times10^{-5}$). Both GOP rates generally peaked concurrently with daily PAR (Fig. S1 in ESM S1). However, the magnitude of hourly GOP_{TOI} tracked hourly fluctuations in PAR more closely than GOP_{O2} did (Fig. 2a–c). This resulted in greater divergence between methods (GOP_{TOI}-GOP_{O2}) with larger changes in PAR within a day ($r = 0.24$, $p = 4\times10^{-2}$; correlation of z scores standardized by day). In part because of this differing sensitivity, the two GOP rates exhibited coarse agreement overall (Fig. 3a; limits of agreement—95% confidence intervals surrounding the mean rate difference—were 15 mmol O_2 m^{-2} h^{-1}, similar to peak midday rates), and GOP_{TOI} was on average slightly greater than GOP_{O2} (GOP_{TOI}-GOP_{O2} = 1.6 mmol O_2 m^{-2} h^{-1}, p = 0.05). This mean difference (bias) was not significant when normalized to the magnitude of production (Fig. 3b; [GOP_{TOI}-GOP_{O2}] / mean [GOP_{TOI}, GOP_{O2}] = 0.1, $p = 3\times10^{-1}$). Despite the lack of major biases in the mean, the rate differences were correlated to the magnitude of GOP in both absolute ($r = 0.35$, $p = 1\times10^{-3}$) and relative terms ($r = 0.23$, $p = 4\times10^{-2}$).

Hourly NEM was autotrophic at midday, but heterotrophic in the morning and evening. Overnight R was relatively constant, despite hourly variability and of similar magnitude to daytime GOP.

Daily rates of GOP_{O2} and GOP_{TOI} (scaled to PAR, "Ecosystem metabolism rate calculations"section; Fig. 2d) were similarly significantly correlated ($r = 0.56$, $p = 1\times10^{-2}$) and in broad agreement (Fig. 3c, d; limits of agreement were 6 mmol O_2 m^{-2} h^{-1}). There was no significant bias between rates (absolute difference 0.2 mmol O_2 m^{-2} h^{-1}, $p = 8\times10^{-1}$; relative difference 0.0, $p = 7\times10^{-1}$) or rate divergence as a function of production (correlation of absolute rate difference to mean GOP: $r = 0.38$, $p = 1\times10^{-1}$; correlation of relative difference: $r = 0.41$, $p = 8\times10^{-2}$). Both GOP_{TOI} and GOP_{O2} followed similar seasonal patterns, with generally increasing rates in May through August and lower rates in mid-September through October.

Daily respiration rates similarly decreased from summer into fall, while daily NEM was relatively constant and heterotrophic over the time series. Large, synchronous decreases in GOP_{O2}, NEM, and R lasting several days were associated with periods of spring tide flooding of the pond. It is unclear whether these rate decreases reflect homogenization of metabolic tracers across the marsh environment during periods of tidal interconnectivity or limitations of the mass balance in the presence of potential lateral fluxes; in either case, GOP_{TOI} was not evaluated during periods of tidal flooding.

Spatial Environmental Heterogeneity

Temperature, O_2 saturation state, the TOI ratios ($^{17}\Delta$), and GOP_{TOI} varied across the pond (Table S1 in ESM S3), particularly along the eastern edge where plant and macroalgal abundance was high. The southernmost portion of the pond also had macroalgal cover (e.g., sample location 4, Fig. 1) but was omitted from weekly surveys to minimize interference with concurrent experiments. The spatial surveys on May 29

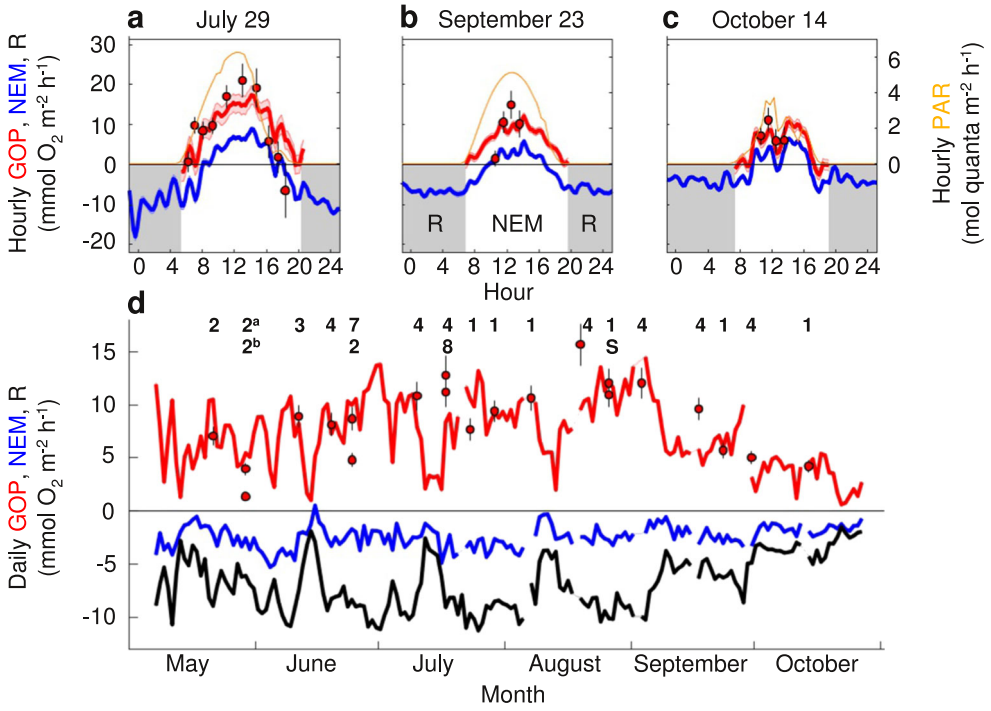

Fig. 2 (color figure online) Hourly and daily ecosystem metabolism rates. Rates of gross oxygen production, GOP_{O2} (red line and shaded one standard deviation error bounds) and GOP_{TOI} (red circles and black one standard deviation error bars), dark respiration and sediment oxygen uptake, *R* (black line and shaded error bounds), and net ecosystem metabolism, NEM (blue line and shaded error bounds). Shaded error bars do not include systematic errors shared by the dissolved oxygen mass balance and triple oxygen isotope methods. (**a–c)** Hourly scale rates plotted against photosynthetically active radiation (PAR, orange line) on 3 days with at least four GOP_{TOI} rates. Here, *R* is inferred to equal average NEM during nighttime periods (grey shaded periods). (**d**) Daily mean rates (same units as **a–c**). Numbers above GOP_{TOI} daily rates indicate the sample location from Fig. 1. GOP_{TOI} daily rates are scaled from at least two midday, hourly scale rates using PAR (see text)

were broadly representative of variability observed across the time series (Fig. 4): In the morning, temperature, O_2 saturation state, and $^{17}\Delta$ were similar around the pond. However, by midday the areas with more vegetation were generally warmer and had higher O_2 saturation state and $^{17}\Delta$. The same areas had greater and more variable rates of dissolved O_2 increases across the time series (Fig. 5; Table S2 in ESM S3). Compared to unvegetated areas, these observations were consistent with increased accumulation of photosynthetic O_2 relative to gas exchange with the atmosphere (Fig. 4), but not necessarily higher production rates (Fig. 2d). While wind speed was generally low, wind direction changed throughout the day, which may have led to temporal and spatial differences in wind-driven gas transfer and water transport that modified the effect of vegetation. In contrast to lateral variability, no vertical gradients in water column properties were detected.

Daily to Seasonal Environmental Variability

Oxygen production covaried with PAR, temperature, tidal stage, and winds over the seasonal time series. In particular, GOP and *R* tracked both short- and long-term variations in PAR and were suppressed by biweekly periods of spring-tide flooding (Fig. S2 in ESM S1) and potential connectivity to the broader marsh (Spivak et al. 2017). The response of GOP, NEM, and *R* to daily to weekly scale environmental variability was evaluated using an ARIMA procedure (Table S3 in ESM S3; the following summary notes significant correlations, $p < 0.05$). GOP_{O2} and *R* were significantly, positively correlated with PAR, and negatively correlated with windspeed and recent tidal flooding. GOP_{O2} was also significantly correlated with wind direction; onshore, westerly winds were associated with greater GOP_{O2}. Onshore winds tend to correspond to fewer clouds and thus higher PAR ($r = 0.31$ for correlation between wind direction and PAR, $p = 4\times10^{-5}$). Neither *R* nor GOP_{O2} was correlated with daily to weekly variability in temperature. Correlations with PAR, winds, and flooding only accounted for 27% of the variance in *R* and 51% of the variance in GOP_{O2}.

In contrast to GOP_{O2}, GOP_{TOI} was not generally correlated with daily to weekly variability in PAR, despite tracking PAR closely at hourly scales, nor was it correlated with the other environmental variables. GOP_{O2} was calculated from *R* and thus these rates were highly cross-correlated ($r = 0.79$, $p = 3\times10^{-26}$), but independently measured GOP_{TOI} was also significantly correlated with *R* ($r = 0.63$, $p = 6\times10^{-3}$). These cross-correlations between GOP and *R* accounted for a greater share of the total variance than accounted for by the measured environmental variables. Thus as yet untested factors may underpin the daily to weekly variability in rates from each

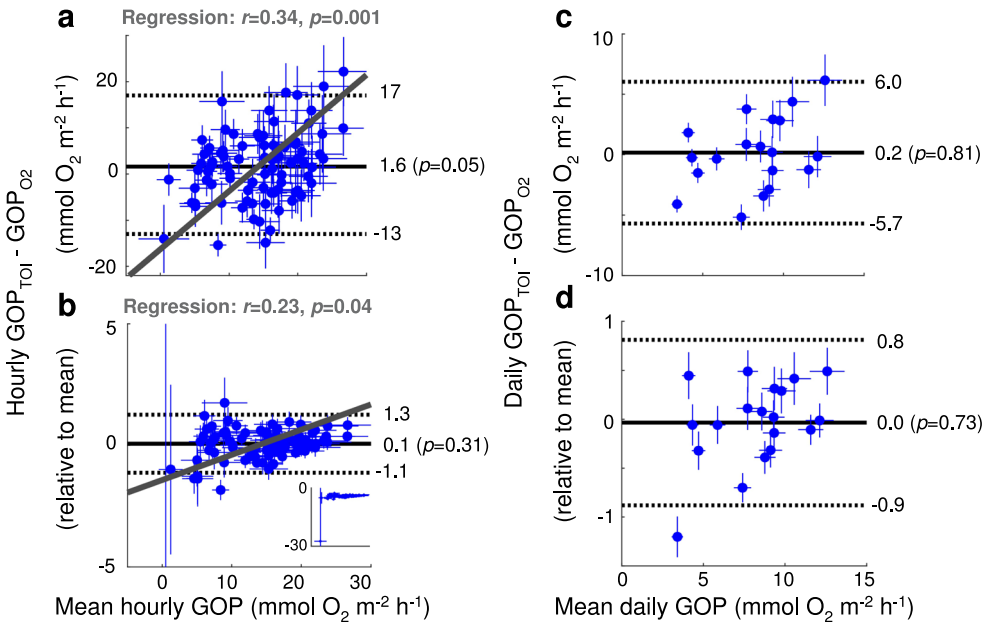

Fig. 3 (color figure online) Gross oxygen production rate comparisons. Differences in (**a**, **b**) hourly and (**c**, **d**) daily rates of gross oxygen production from the triple oxygen isotope and dissolved oxygen mass balance methods (GOP_{TOI} and GOP_{O2}), plotted against the average GOP rate from both methods over concurrent periods. Individual daily or hourly rate differences are plotted as either absolute (GOP_{TOI}-GOP_{O2}, mmol O_2 m^{-2} h^{-1} for either period) or relative differences ([GOP_{TOI}–GOP_{O2}] / mean[GOP_{TOI}, GOP_{O2}]). One standard deviation error bars are in blue. Mean GOP_{TOI}–GOP_{O2} rate difference (bias) is marked with a solid black line (*p* value noted for null hypothesis of no bias), and 95% confidence intervals (limits of agreement) with dashed black lines. Both the absolute and relative hourly rate differences are significantly correlated to the magnitude of production (grey lines and text, with reported *p* reported for linear regression with null hypothesis of no correlation), while the daily rates are not (see text in panels for *r* and *p*). In the inset (**b**), the near zero rate leads to large divergence (–27 relative difference) and relative errors (standard deviation of 193) despite the good constraints on the absolute rate. Because this reflects numerical rather than methodological uncertainty, this point is not included in the calculation of bias, limits of agreement, or the regression of relative rate differences against mean GOP. Including this relative rate does not alter the conclusions

method—ebullition is one likely driver of differences between the two methods over daily time scales (Howard et al. 2018). However, an important caveat is that daily GOP_{TOI} rates were evaluated over only 10% of the overall time series (17 of 174 days), limiting our statistical power.

Discussion

Convergent Rates of Daily to Seasonal GOP

Mean daily rates of GOP_{TOI} and GOP_{O2} broadly agreed over the time series, with similar seasonal trends (Fig. 2d) and no significant bias (Fig. 3c). The mean ratio of GOP_{TOI}/GOP_{O2} = 1.0(0.4). This is similar to the mean and range of ratios calculated in pelagic ocean Lagrangian experiments (Hamme et al. 2012) and estuarine benthic chambers (Stanley and Howard 2013). This agreement implies that even in a setting expected to favor light-dependent O_2 uptake, the contributions of such processes at daily to seasonal time scales are not large compared to the relative methodological uncertainties (on average, 10% of GOP).

There were exceptions to this broad agreement. Eight of the daily GOP_{TOI} rates (Fig. 2d) differed from GOP_{O2} by a larger degree than could be explained by methodological uncertainties (> 2 standard deviations). However, these differences were not consistent with a major role for light-dependent O_2 uptake; larger GOP differences were not systematically distributed over the time series with respect to seasonal trends or daily changes in PAR. Instead, environmental heterogeneity associated with vegetation likely contributed to periods with larger than expected rate differences between GOP_{TOI} at the sample locations and GOP_{O2} at the sensor location.

Temperature and O_2 varied by tens of percent around the pond margins, suggesting that this setting was not always well-mixed despite the lack of vertical gradients. Submerged aquatic vegetation reduces turbulence and increases mixing time scales (Koch and Gust 1999; Romano et al. 2003; Nepf and Ghisalberti 2008). In addition, *U. intestinalis* mats likely limited air-water gas exchange (e.g., Wollenberg and Peters 2009; Attermeyer et al. 2016) and enhanced accumulation of photosynthetic oxygen compared to unvegetated areas. Vegetation likely also contributed to variability in important O_2 sinks in this pond such as ebullition from photosynthetic surfaces (Howard et al. 2018) and the sedimentary uptake dominating the net metabolism of the pond (e.g., sulfide oxidation; Spivak et al. 2018). Thus we infer that the heterogeneity in vegetation cover, and resulting biological and

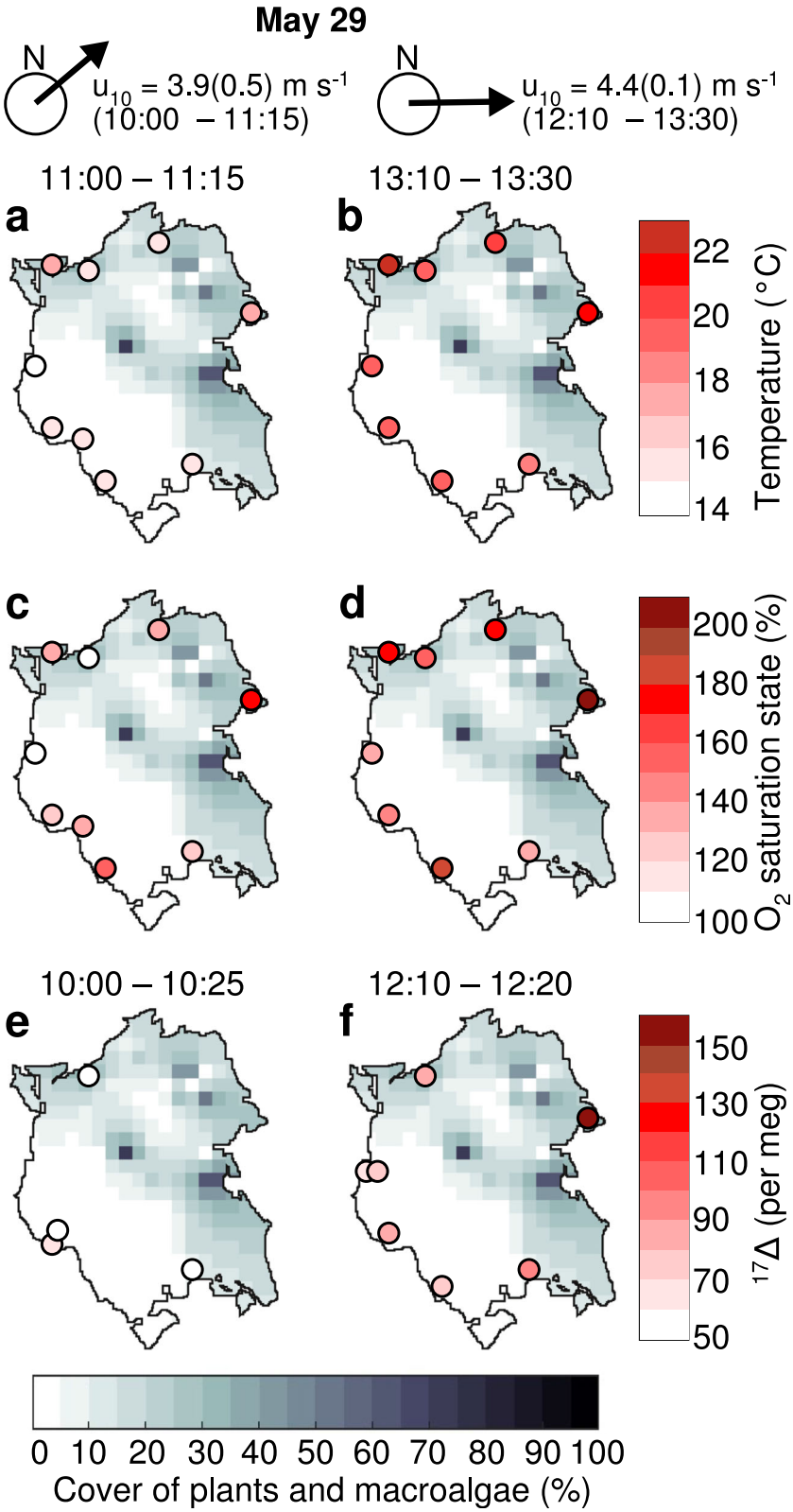

Fig. 4 (color figure online) Spatial variability of temperature, oxygen, and triple oxygen isotope ratios. Morning (left column) and afternoon (right column) values of environmental variables around the pond (filled, colored circles) on May 29 2014, superimposed on vegetation cover map (grayscale). Mean wind direction and speed (standard deviation in parentheses) for each period is followed by **(a**, **b)** temperature, **(c**, **d**) dissolved oxygen saturation relative to atmospheric equilibrium, and **(e**, **f**) the triple oxygen isotope tracer of oxygen derived from photosynthesis relative to air-water gas exchange, $^{17}\Delta$

physical impacts on O_2 dynamics, contributed to variability in production rates around the pond. In larger lakes, spatial heterogeneity in temperature and oxygen can lead to highly variable estimates of gross productivity and respiration (Van de Bogert et al. 2012), and submerged aquatic vegetation strongly influences these environmental drivers (Vilas et al.

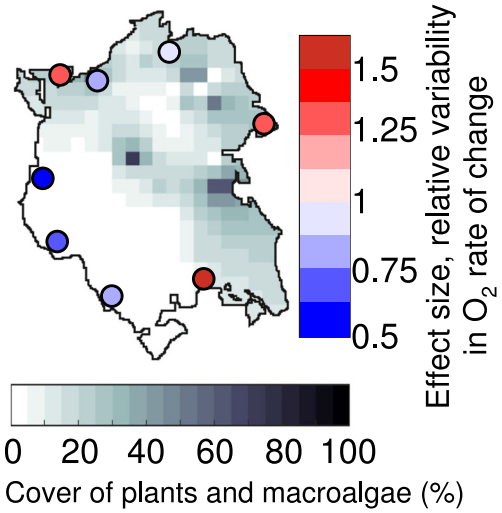

Fig. 5 (color figure online) Seasonal variability in dissolved oxygen rate of increase. Effect size of variability in rate of morning to afternoon increase in dissolved oxygen saturation state, across all spatial surveys over the sampling season (see text), overlaid on map of vegetation cover. An effect size of 0.5 means that, compared to the mean across the pond, oxygen increases at a given sample location were 50% less variable over the sampling season. More vegetated areas of the pond generally had greater variability in daily rates of increase, as well as larger daily increases (Table S2 in ESM S3)

2017). This is also consistent with the important role of vegetation cover in explaining variability in metabolism rates between salt marsh ponds (Spivak et al. 2017).

Light-Dependent Effects on Rates of Hourly GOP

In contrast to the daily rates, there were systematic discrepancies in hourly rates of GOP_{TOI} and GOP_{O2} during midday periods which could reflect light-dependent processes. There was a small but significant bias between GOP_{TOI} and GOP_{O2} (Figs. 2a–c and 3a). This resulted in a ratio of hourly GOP_{TOI}/GOP_{O2} equal to 1.4(1.7). The variability in this ratio was increased compared to daily rates in part because of the large relative uncertainty associated with near-zero dawn and dusk GOP rates; the ratio derived from only the highest production rate on each day was 1.5(0.6). This poorer agreement during periods of peak production was not a function of lags between the GOP rates—instead, the GOP_{TOI}-GOP_{O2} difference was correlated with hourly fluctuations in the magnitude of production and PAR (see "Metabolic Rate Comparison" section). These relationships point to a potential small but observable divergence of hourly GOP rates due to light-dependent O_2 uptake. The greater GOP_{TOI} relative to GOP_{O2} was consistent with the expected effects of plausible light-dependent processes (Table 1), and within the range of the 23–62% difference expected if light-dependent O_2 uptake were two to ten times greater than in the dark (e.g., Bender et al. 1987; Epping and Jørgensen 1996; Pringault et al. 2009). This ratio was greater than could be explained by the expected uncertainties in the difference between hourly rates (on average, 16% of GOP).

Daytime oxidation of reduced compounds produced overnight in the sediments (Fenchel and Glud 2000) is likely in shallow pond sediments, but would be expected to cause GOP rates to diverge most in the morning. Photorespiration would cause GOP rates to diverge most in the afternoon when the ratio of O_2 to carbon dioxide is highest in this pond (Howard 2017) and nearby shallower pools (Koop-Jakobsen and Gutbrod 2019). Instead, the GOP_{TOI}-GOP_{O2} difference is greatest at peak production and PAR. Light-stimulation of mitochondrial respiration can cause GOP_{O2} to underestimate productivity, and contributes to both autotrophic and heterotrophic carbon metabolism at ecosystem scales (Grande et al. 1989; Pringault et al. 2009). In contrast, photoreduction, or the Mehler reaction, is largely decoupled from carbon metabolism (Williams and del Giorgio 2005), and may primarily serve to remove excess electrons at the cellular level (Raven and Beardall 2005). Photoreduction reduces O_2 to water at photosystem I (PSI), and can be a major oxygen uptake flux for autotrophs in the light, consuming the equivalent of 10–75% of photosystem II (PSII) O_2 output (Milligan et al. 2007; Halsey et al. 2010; Roberty et al. 2014) and causing GOP_{TOI} to overestimate productivity. Both processes could lead to the observed midday divergence between GOP_{TOI} and GOP_{O2} (ESM S1).

However, as with the daily GOP rates, environmental heterogeneity at hourly scales may play a large role in this setting, and the limited spatial resolution across the pond makes it difficult to confirm that the observed differences at short time scales are mainly due to light-dependent processes. Ebullition in particular, where active, may lead to divergent GOP_{O2} and GOP_{TOI} in the midday and afternoon when most bubbles escape (Howard et al. 2018).

Daytime Production and Net Ecosystem Metabolism

The pond in this study was shallow and heterotrophic on daily to seasonal time scales, but autotrophic during the daytime. This metabolic dynamism may contribute to our seemingly contradictory findings of a potential role of light-dependent O_2 uptake over short periods during autotrophic daytime periods, but no effect over daily to seasonal periods; large, light-insensitive respiration rates could mask smaller light-dependent fluxes when integrated over longer time periods. Midday (~ 3 h) chamber experiments found lower rates of respiration and a more autotrophic balance of production and respiration in surface waters than in chambers overlying sediments (Howard 2017). GOP_{TOI} and GOP_{O2} agreed in chambers over microalgae and macroalgae covered sediments, and the metabolism of suspended microalgae was minor compared to sedimentary fluxes. Thus, potential light-

dependent differences may arise from portions of the pond with *R. maritima*.

Prior work in this and other salt marsh ponds showed that organic-rich sediments support high rates of ecosystem respiration (Spivak et al. 2017), through both aerobic and anaerobic pathways including microbial sulfur cycling (Wilbanks et al. 2014; Rao et al. 2016; Spivak et al. 2018). Thus, reduced compounds in pond sediments have the potential to consume much of the O_2 produced during daytime periods of water column autotrophy. This point is illustrated by comparing ratios of NEM/GOP (Fig. 6); during daylight periods ratios were ~ 0 (using GOP from either method), indicating that as much O_2 was consumed as was produced. Over 24 h, nighttime O_2 uptake pushed the system to net heterotrophy (NEM/GOP ~ − 0.4, i.e., respiration exceeded production by 40%). The net result that NEM varied little over the six month study period (Fig. 2d) is underlain by a steady background of sedimentary O_2 uptake. Concurrent assessments of microbial activity in this pond also point to more stable sediment conditions compared to the overlying water column; microbial activity in the water column was strongly associated with diel changes in environmental conditions, but microbial communities in surficial sediments were insensitive to changes in overlying temperature and O_2 (Kearns et al. 2017).

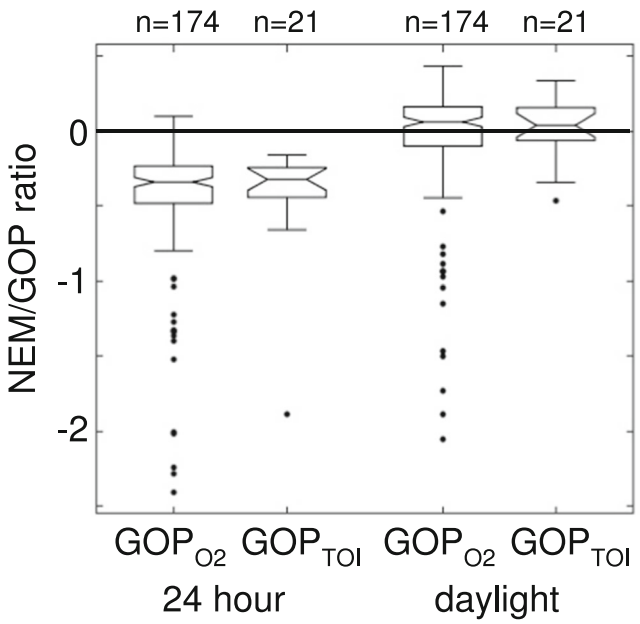

Fig. 6 Net to gross productivity ratios. The ratio of dissolved oxygen-based net ecosystem metabolism (NEM) to gross oxygen production derived from either a dissolved oxygen diel mass balance or the triple oxygen isotope method (GOP_{O2} or GOP_{TOI}). The two leftmost boxes represent the range of observed 24 h NEM/GOP ratios (including night and day), while the two rightmost boxes represent daytime NEM/GOP ratios (dawn to dusk). A value of zero (thick horizontal line) indicates no net consumption or storage of primary production in the system, while a negative value indicates net heterotrophy. Box heights represent the interquartile ranges of data, upper box whiskers encompass maximum observed ratios, lower box whiskers are 1.5 times the interquartile length, and individual points represent observations more negative than the lower whisker, encompassing the bottom 4–8% of the data. Thin horizontal lines within the boxes indicate the median of observations, and notch height represents the 95% confidence interval in the median—overlapping notches indicate medians are not significantly different for NEM/GOP_{O2} and NEM/GOP_{TOI}

Conclusions

The TOI method was expected to highlight light-dependent processes that could affect GOP estimates from dissolved O_2 mass balances. On daily to seasonal time scales, we found good overall agreement between daily to seasonal rates GOP_{TOI} and GOP_{O2}, despite a number of environmental factors expected to cause light-dependent O_2 uptake. This agreement may reflect the strong heterotrophy and dominance of sedimentary respiration in this shallow pond, which consumed more O_2 than photosynthetically produced.

Hourly GOP rates within individual days did exhibit discrepancies between the methods that were consistent with light-dependent processes. Given the ambiguous importance of light-dependent O_2 uptake in this setting, we could not disentangle the potential light-dependent processes affecting our results. However, photoreduction and light-stimulated mitochondrial respiration are likely processes in this setting that are consistent with the observed O_2 dynamics.

Ultimately, the importance of daily to seasonal agreement (or hourly disagreement) between the TOI and dissolved O_2 mass balance methods depends upon the research question. The hourly time series in this study point to isotopic method having sufficient resolution to study light-dependent O_2 uptake processes in a common O_2 currency with a dissolved mass balance. In a setting with smaller respiratory fluxes these differences would be proportionally larger, which could contribute to the high ratios of light versus dark respiration reported for other environments (e.g., Bender et al. 1987). However, the typical use of dissolved O_2 mass balances is to study ecosystem metabolism fluxes over daily to yearly time scales. In this salt marsh pond, the daily production rates derived from the TOI method agreed with those from the dissolved O_2 mass balance. Our results support the typical assumption that daytime and nighttime rates of O_2 consumption rates are similar, at least in environments where light-independent sediment respiration dominates ecosystem metabolism. Thus we view the TOI method, with additional analytical requirements, as being best suited for targeted process studies rather than routine monitoring in aquatic environments in which dissolved O_2 sensors can be readily deployed and maintained. For pelagic locations where instrumentation is not practical (e.g., infrequently occupied hydrographic stations), this work suggests that the TOI method can provide a good alternative for evaluating in situ oxygen production.

The heterogeneity of production over small spatial scales around this small pond is an important additional finding. This contributes to the growing understanding that even very shallow aquatic environments may not be well-mixed (e.g., Holgerson et al. 2016), which can complicate interpretation of biogeochemical tracers and drive substantial spatial heterogeneity in metabolic rates (Van de Bogert et al. 2012).

Acknowledgments Ancillary meteorological data are accessible from the LTER Network Information System Data Portal (https://doi-org/10.6073/pasta/14eb405f583ae2384b2c6c5714776214). The dissolved oxygen and other environmental time series collected from sensor deployments are accessible from the Biological and Chemical Oceanography Data Management Office (https://www.bco-dmo.org/dataset/670819). Other data used in this work (e.g., isotopic ratios) are provided in the supplementary materials available with the electronic version of this paper.

Authors' contributions E.M.H., A.C.S., and R.H.R.S. developed the isotopic time series study. E.M.H. and A.C.S. wrote the manuscript. All authors contributed to sample collection, sample analysis, and/or data interpretation, and commented on manuscript drafts. The authors declare that they have no conflict of interest.

Funding Information This work depended on the outstanding logistical and in-kind support of the Plum Island Ecosystems Long-Term Ecological Research site and TIDE experiment staff and scientists (National Science Foundation (NSF) OCE 1238212, NSF DEB 1354494, and Northeast Climate Science Center grant DOI G12-AC00001). We thank Nancy Pau and the Parker River National Wildlife Refuge for permitting, and Jeanine Ash and one anonymous reviewer for thoughtful feedback on the manuscript. E.M.H. was supported by the National Defense Science and Engineering Graduate Fellowship. Funding for this research and support for A.C.S. and R.H.R.S. was provided by NSF OCE 1233678. Additional support to A.C.S was provided by Woods Hole Sea Grant (NA14OAR4170104) and the National Oceanic and Atmospheric Administration and National Estuarine Research Reserve System Science Collaborative (NA14NOS4190145). J.S.K. was supported by the Woods Hole Oceanographic Institution (WHOI) Summer Student Fellowship program.

References

Abe, O., and N. Yoshida. 2003. Partial pressure dependency of $^{17}O/^{16}O$ and $^{18}O/^{16}O$ of molecular oxygen in the mass spectrometer. *Rapid Communications in Mass Spectrometry* 17 (5): 395–400. https://doi.org/10.1002/rcm.923.

Angert, A., S. Rachmilevitch, E. Barkan, and B. Luz. 2003. Effects of photorespiration, the cytochrome pathway, and the alternative pathway on the triple isotopic composition of atmospheric O_2. *Global Biogeochemical Cycles* 17 (1): 1030. https://doi.org/10.1029/2002GB00193.

Ash, J.L., H. Hu, and L.Y. Yeung. 2020. What Fractionates Oxygen Isotopes during Respiration? Insights from Multiple Isotopologue Measurements and Theory. *ACS Earth and Space Chemistry* 4 (1): 50-66. https://doi.org/10.1021/acsearthspacechem.9b00230

Attermeyer, K., S. Flury, R. Jayakumar, P. Fiener, K. Steger, V. Arya, F. Wilken, R. van Geldern, and K. Premke. 2016. Invasive floating macrophytes reduce greenhouse gas emissions from a small tropical lake. *Scientific Reports* 6: 20424. https://doi.org/10.1038/srep20424.

Bender, M., J. Orchardo, M-L. Dickson, R. Barber, and S. Lindley. 1999. In vitro O_2 fluxes compared with ^{14}C production and other rate terms during the JGOFS Equatorial Pacific experiment. *Deep Sea Research I* 46(4): 637-654. https://doi.org/10.1016/S0967-0637(98)00080-6

Bender, M., K. Grande, K. Johnson, J. Marra, P.J.L.B. Williams, J. Sieburth, M. Pilson, C. Langdon, G. Hitchcock, J. Orchardo, C. Hunt, P. Donaghay, and K. Heinemann. 1987. A comparison of four different methods for determining planktonic community production. *Limnology and Oceanography* 32 (5): 1085–1098. https://doi.org/10.4319/lo.1987.32.5.1085.

Benson, B.B., and D. Krause Jr. 1980. The concentration and isotopic fractionation of gases dissolved in freshwater in equilibrium with the atmosphere: 1. *Oxygen. Limnol. Oceanogr.* 25 (4): 662–671. https://doi.org/10.4319/lo.1980.25.4.0662.

Benson, B.B., and D. Krause Jr. 1984. The concentration and isotopic fractionation of oxygen dissolved in freshwater and seawater in equilibrium with the atmosphere. *Limnology and Oceanography* 29 (3): 620–632. https://doi.org/10.4319/lo.1984.29.3.0620.

Buapet, P., L.M. Rasmusson, M. Gullström, and M. Björk 2013. Photorespiration and carbon limitation determine productivity in temperate seagrasses.

Caffrey, J.M. 2004. Factors controlling net ecosystem metabolism in U.S. estuaries. Estuar. *Coasts* 27 (1): 90–101. https://doi.org/10.1007/BF02803563.

D'Errico, J. 2012. inpaint_nans v.1.1. Matlab File Exchange. https://www.mathworks.com/matlabcentral/fileexchange/4551-inpaint_nans. Accessed 1 Aug 2017.

Demars, B.O.L., J. Thompson, and J.R. Manson. 2015. Stream metabolism and the open diel oxygen method: Principles, practice, and perspectives. *Limnology and Oceanography: Methods* 13 (7): 356–374. https://doi.org/10.1002/lom3.10030.

Eisenstadt, D., E. Barkan, B. Luz, and A. Kaplan. 2010. Enrichment of oxygen heavy isotopes during photosynthesis in phytoplankton. *Photosynthesis Research* 103: 97–103. https://doi.org/10.1007/s11120-009-9518-z.

Epping, E.H.G., and B.B. Jørgensen. 1996. Light-enhanced oxygen respiration in benthic phototrophic communities. *Marine Ecology Progress Series* 139: 193–203. https://doi.org/10.3354/meps139193.

Falkowski, P.G., and T.G. Owens. 1978. Effects of light intensity on photosynthesis and dark respiration in six species of marine phytoplankton. *Marine Biology* 45 (4): 289–295. https://doi.org/10.1007/BF00391815.

Falkowski, P.G., and J.A. Raven. 1997. *Aquatic photosynthesis*. Paris: Blackwell Science.

Fenchel, T., and R.N. Glud. 2000. Benthic primary production and O_2-CO_2 dynamics in a shallow-water sediment: Spatial and temporal heterogeneity. *Ophelia* 53 (2): 159–171. https://doi.org/10.1080/00785236.2000.10409446.

Forbrich, I., and A.E. Giblin. 2015. Marsh-atmosphere CO_2 exchange in a New England salt marsh. *Journal of Geophysical Research – Biogeosciences* 120 (9): 1825–1838. https://doi.org/10.1002/2015JG003044.

Garcia, H.E., and L.I. Gordon. 1992. Oxygen solubility in seawater: Better fitting equations. *Limnology and Oceanography* 37 (6): 1307–1312. https://doi.org/10.4319/lo.1992.37.6.1307.

Garcia, H.E., and L.I. Gordon. 1993. Erratum: Oxygen solubility in seawater: Better fitting equations. *Limnology and Oceanography* 38 (3): 656. https://doi.org/10.4319/lo.1993.38.3.0643.

Grande, K.D., J. Marra, C. Langdon, K. Heinemann, and M.L. Bender. 1989. Rates of respiration in the light measured in marine phytoplankton using an ^{18}O isotope-labeling technique. *Journal of Experimental Marine Biology and Ecology* 129 (2): 95–120. https://doi.org/10.1016/0022-0981(89)90050-6.

Halsey, K.H., A.J. Milligan, and M.J. Behrenfeld. 2010. Physiological optimization underlies growth rate-independent chlorophyll-specific gross and net primary production. *Photosynthesis Research* 103 (2): 125–137. https://doi.org/10.1007/s11120-009-9526-z.

Hamme, R.C., N. Cassar, V.P. Lance, R.D. Vaillancourt, M.L. Bender, P.G. Strutton, T.S. Moore, M.D. DeGrandpre, C.L. Sabine, D.T. Ho, and B.R. Hargreaves. 2012. Dissolved O_2/Ar and other methods reveal rapid changes in productivity during a Lagrangian experiment in the Southern Ocean. *Journal of Geophysical Research, Oceans* 117 (C00F12): 1–19. https://doi.org/10.1029/2011JC007046.

Helman, Y., E. Barkan, D. Eisenstadt, and A. Kaplan. 2005. Fractionation of the three stable oxygen isotopes by oxygen-producing and oxygen-consuming reactions in photosynthetic organisms. *Plant Physiology* 138 (4): 2292–2298. https://doi.org/10.1104/pp.105.063768.

Holgerson, M.A., C.J. Zappa, and P.A. Raymond. 2016. Substantial overnight reaeration by convective cooling discovered in pond ecosystems. *Geophysical Research Letters* 43 (15): 8044–8051. https://doi.org/10.1002/2016GL070206.

Holtgrieve, G.W., D.E. Schindler, T.A. Branch, and Z.T. A'mar. 2010. Simultaneous quantification of aquatic metabolism and reaeration using a Bayesian statistical model of oxygen dynamics. *Limnology and Oceanography* 55 (3): 1047–1063. https://doi.org/10.4319/lo.2010.55.3.1047.

Howard, E.M. 2017. Ecosystem metabolism in salt marsh tidal creeks and ponds: Applying triple oxygen isotopes and other gas tracers to novel environments, pp. 69–70, 135–172. Woods Hole, MA: PhD thesis submitted to the Massachusetts Institute of Technology and the Woods Hole Oceanographic Institution. https://doi.org/10.1575/1912/8654

Howard, E.M., I. Forbrich, A.E. Giblin, D.E. Lott III, K.L. Cahill, and R.H.R. Stanley. 2018. Using noble gases to compare parameterizations of air-water gas exchange and to constrain oxygen losses by ebullition in a shallow aquatic environment. *Journal of Geophysical Research – Biogeosciences* 123 (9): 2711–2726. https://doi.org/10.1029/2018JG004441.

Juranek, L.W., and P.D. Quay. 2013. Using triple isotopes of dissolved oxygen to evaluate global marine productivity. *Annual Review of Marine Science* 5: 503–524. https://doi.org/10.1146/annurev-marine-121211-172430.

Kaiser, J. 2011. Technical note: Consistent calculation of aquatic gross production from oxygen triple isotope measurements. *Biogeosci.* 8 (7): 1793–1811. https://doi.org/10.5194/bg-8-1793-2011.

Kaiser, J., and O. Abe. 2012. Reply to Nicholson's comment on "Consistent calculation of aquatic gross production from oxygen triple isotope measurements" by Kaiser (2011). *Biogeosci* 9 (8): 2993–2997. https://doi.org/10.5194/bg-8-2993-2011.

Kana, T.M. 1990. Light-dependent oxygen cycling measured by an oxygen-18 isotope dilution technique. *Marine Ecology Progress Series* 64: 293–300. https://doi.org/10.3354/meps064293.

Kearns, P.J., D. Holloway, H.H. Angell, S.G. Feinman, and J.L. Bowen. 2017. Effect of short-term, diel changes in environmental conditions on active microbial communities in a salt marsh pond. *Aquatic Microbial Ecology* 80 (1): 29–41. https://doi.org/10.3354/ame01837.

Keeling, R.F., A.C. Manning, E.M. McEvoy, and S.R. Shertz. 1998. Methods for measuring changes in atmospheric O_2 concentration and their application in southern hemisphere air. *Journal of Geophysical Research* 103 (D3): 3381–3397. https://doi.org/10.1029/97JD02537.

Koch, E.W., and G. Gust. 1999. Water flow in tide- and wave-dominated beds of the seagrass *Thalassia testudinum*. *Marine Ecology Progress Series* 184: 63–72. https://doi.org/10.3354/meps184063.

Koop-Jakobsen, K., and M.S. Gutbrod. 2019. Shallow salt marsh tidal ponds—an environment with extreme oxygen dynamics. *Frontiers in Environmental Science* 7 (137): 1–14. https://doi.org/10.3389/fenvs.2019.00137.

Laws, E.A., M.R. Landry, R.T. Barber, L. Campbell, M-L. Dickson, and J. Marra. 2000. Carbon cycling in primary production bottle incubations: inferences from grazing experiments and photosynthetic studies using ^{14}C and ^{18}O in the Arabian Sea. Deep Sea Research, Part II 47(7): 1339–1352. https://doi.org/10.1016/S0967-0645(99)00146-0

Li, B., L.Y. Yeung, H. Hu, and J.L. Ash. 2019. Kinetic and equilibrium fractionation of O_2 isotopologues during air-water gas transfer and implications for tracing oxygen cycling in the ocean. *Marine Chemistry* 210: 61–71. https://doi.org/10.1016/j.marchem.2019.02.006.

Luz, B., and E. Barkan. 2000. Assessment of oceanic productivity with the triple-isotope composition of dissolved oxygen. *Science* 288 (5473): 2028–2031. https://doi.org/10.1126/science.288.5473.2028.

Luz, B., and E. Barkan. 2005. The isotopic ratios $^{17}O/^{16}O$ and $^{18}O/^{16}O$ in molecular oxygen and their significance in biogeochemistry. *Geochimica et Cosmochimica Acta* 69 (5): 1099–1110. https://doi.org/10.1016/j.gca.2004.09.001.

Luz, B., and E. Barkan. 2011. Proper estimation of marine gross O_2 production with $^{17}O/^{16}O$ and $^{18}O/^{16}O$ ratios of dissolved O_2. *Geophysical Research Letters* 38 (19): L19606. https://doi.org/10.1029/2011GL049138.

Manning, C.C., and E.M. Howard. 2017. calcGOP: Functions for calculating gross oxygen production from measurements of the triple oxygen isotopic composition of dissolved O_2. http://github.com/caramanning/calcGOP, release 1.0.

Manning, C.C., E.M. Howard, D.P. Nicholson, B.Y. Ji, Z.O. Sandwith, and R.H.R. Stanley. 2017. Revising estimates of aquatic gross oxygen production by the triple oxygen isotope method to incorporate the local isotopic composition of water. *Geophysical Research Letters* 44 (20): 10511–10519. https://doi.org/10.1002/2017GL074375.

Milligan, A.J., I. Berman-Frank, Y. Gerchman, G.C. Dismukes, and P.G. Falkowski. 2007. Light-dependent oxygen consumption in nitrogen-fixing cyanobacteria plays a key role in nitrogenase protection. *Journal of Phycology* 43 (5): 845–852. https://doi.org/10.1111/j.1529-8817.2007.00395.x.

Nepf, H., and M. Ghisalberti. 2008. Flow and transport in channels with submerged vegetation. *Acta Geophsica* 56 (3): 753–777. https://doi.org/10.2478/s11600-008-0017-y.

Nicholson, D.P. 2011. Comment on: "Technical note: Consistent calculation of aquatic gross production from oxygen triple isotope measurements" by Kaiser (2011). *Biogeosci.* 8 (10): 2993–2997. https://doi.org/10.5194/bg-8-2993-2011.

Odum, H.T. 1956. Primary production in flowing waters. *Limnology and Oceanography* 1 (2): 102–117. https://doi.org/10.4319/lo.1956.1.2.0102.

Parkhill, K.L., and J.S. Gulliver. 1998. Application of photorespiration concepts to whole stream productivity. *Hydrobiologia* 389 (1): 7–19. https://doi.org/10.1023/A:1003519302002.

Pringault, O., S. Tesson, and E. Rochelle-Newall. 2009. Respiration in the light and bacterio-phytoplankton coupling in a coastal environment. *Microbial Ecology* 57 (2): 321–334. https://doi.org/10.1007/s00248-008-9422-7.

Prokopenko, M.G., O.M. Pauluis, J. Granger, and L.Y. Yeung. 2011. Exact evaluation of gross photosynthetic production from the oxygen triple-isotope composition of O_2: Implications for the net-to-gross primary production ratios. *Geophysical Research Letters* 38 (14): L14603. https://doi.org/10.1029/2011GL047652.

Rao, A., N. Risgaard-Petersen, and U. Neumeier. 2016. Electrogenic sulfur oxidation in a northern saltmarsh (St. Lawrence Estuary, Canada). *Canadian Journal of Microbiology* 62 (6): 530–537. https://doi.org/10.1139/cjm-2015-0748.

Raven, J.A., J. Beardall. 2005. Respiration in aquatic photolithotrophs. In: del Giorgio P and Williams P (eds) *Respiration in Aquatic Ecosystems*, pp. 36–46. Oxford: Oxford University Press.

Reuer, M.K., B.A. Barnett, M.L. Bender, P.G. Falkowski, and M.B. Hendricks. 2007. New estimates of Southern Ocean biological production rates from O_2/Ar ratios and the triple isotope composition of O_2. *Deep Sea Research, Part I* 54 (6): 951–974. https://doi.org/10.1016/j.dsr.2007.02.007.

Roberty, S., B. Bailleul, N. Berne, F. Franck, and P. Cardol. 2014. PSI Mehler reaction is the main alternative photosynthetic electron pathway in Symbiodinium sp., symbiotic dinoflagellates of cnidarians. *New Phytologist* 204 (1): 81–91. https://doi.org/10.1111/nph.12903.

Romano, C., J. Widdows, M.D. Brinsley, and F.J. Staff. 2003. Impact of *Enteromorpha intestinalis* mats on near-bed currents and sediment dynamics: Flume studies. *Marine Ecology Progress Series* 256: 63–74. https://doi.org/10.3354/meps256063.

Sarma, V.V.S.S., O. Abe, S. Hashimoto, A. Hinuma, and T. Saino. 2005. Seasonal variations in triple oxygen isotopes and gross oxygen production in the Sagami Bay, central Japan. *Limnology and Oceanography* 50 (2): 544–552. https://doi.org/10.4319/lo.2005.50.2.0544.

Spivak, A.C., K. Gosselin, E.M. Howard, G. Mariotti, I. Forcrich, R.H.R. Stanley, and S.P. Sylva. 2017. Shallow ponds are heterogeneous habitat within a temperate salt marsh ecosystem. *Journal of Geophysical Research – Biogeosciences* 122 (6): 1371–1384. https://doi.org/10.1002/2017JG003780.

Spivak, A.C., K. Gosselin, and S.P. Sylva. 2018. Shallow ponds are biogeochemically distinct habitats in salt marsh ecosystems. *Limnology and Oceanography* 63 (4): 1622–1643. https://doi.org/10.1002/lno.10797.

Staehr, P.A., D. Bade, M.C. Van de Bogert, G.R. Koch, C. Williamson, P. Hanson, J.J. Cole, and T. Kratz. 2010. Lake metabolism and the diel oxygen technique: State of the science. *Limnology and Oceanography: Methods* 8 (11): 628–644. https://doi.org/10.4319/lom.2010.8.0628.

Stanley, R.H.R., and E.M. Howard. 2013. Quantifying photosynthetic rates of microphytobenthos using the triple isotope composition of dissolved oxygen. *Limnology and Oceanography: Methods* 11: 360–373. https://doi.org/10.4319/lom.2013.11.360.

Stanley, R.H.R., J.B. Kirkpatrick, N. Cassar, B.A. Barnett, and M.L. Bender. 2010. Net community production and gross primary production rates in the western equatorial Pacific. *Global Biogeochemical Cycles* 24 (4): GB4001. https://doi.org/10.1029/2009GB003651.

Suggett, D.J., H.L. MacIntyre, T.M. Kana, and R.J. Geider. 2009. Comparing electron transport with gas exchange: Parameterising exchange rates between alternative photosynthetic currencies for eukaryotic phytoplankton. *Aquatic Microbial Ecology* 56: 147–162. https://doi.org/10.3354/ame01303.

Thiemens, M.H. 2001. The mass-independent ozone isotope effect. *Science* 293 (5528): 226. https://doi.org/10.1126/science.1063648.

Vachon, D., and Y.T. Prairie. 2013. The ecosystem size and shape dependence of gas transfer velocity versus wind speed relationships in lakes. *Canadian Journal of Fisheries and Aquatic Sciences* 70 (12): 1757–1764. https://doi.org/10.1139/cjfas-2013-0241.

Van de Bogert, M.C., D.L. Bade, S.R. Carpenter, J.J. Cole, M.L. Pace, P.C. Hanson, and O.C. Langman. 2012. Spatial heterogeneity strongly affects estimates of ecosystem metabolism in two north temperate lakes. *Limnology and Oceanography* 57 (6): 1689–1700. https://doi.org/10.4319/lo.2012.57.6.1689.

Vilas, M.P., C.L. Marti, M.P. Adams, C.E. Oldham, and M.R. Hipsey. 2017. Invasive macrophytes control the spatial and temporal patterns of temperature and dissolved oxygen in a shallow lake: A proposed feedback mechanism of macrophytes loss. *Frontiers in Plant Science* 8: 2097. https://doi.org/10.3389/fpls.2017.02097.

Wilbanks, E.G., U. Jaekel, V. Salman, P.T. Humphrey, J.A. Eisen, M.T. Facciotti, D.H. Buckley, S.H. Zinder, G.K. Druschel, D.A. Fike, and V.J. Orphan. 2014. Microscale sulfur cycling in the phototrophic pink berry consortia of the Sippewissett Salt Marsh. *Environmental Microbiology* 16 (11): 3398–3415. https://doi.org/10.1111/1462-2920.12388.

Williams, P.J. Le B., and P.A. del Giorgio. 2005. Respiration in aquatic ecosystems: history and background. In: del Giorgio P and Williams P (eds) *Respiration in Aquatic Ecosystems*, 1–17. Oxford: Oxford University Press.

Winslow, L.A., J.A. Zwart, R.D. Batt, H.A. Dugan, R.I. Woolway, J.R. Corman, P.C. Hanson, and J.S. Read. 2016. LakeMetabolizer: an R package for estimating lake metabolism from free-water oxygen using diverse statistical models. *Inland Waters* 6 (4): 622–636. https://doi.org/10.5268/IW-6.4.883.

Wollenberg, J.L., and S.C. Peters. 2009. Diminished mercury emission from waters with duckweed cover. *Journal of Geophysical Research – Biogeosciences* 114 (G2): G00C08. https://doi.org/10.1029/2008JG000770.

Yang, B., S.R. Emerson, and S.M. Bushinsky. 2017. Annual net community production in the subtropical Pacific Ocean from *in situ* oxygen measurements on profiling floats. *Global Biogeochemical Cycles* 31 (4): 728–744. https://doi.org/10.1002/2016GB005545.

Yvon-Durocher, G., J.M. Caffrey, A. Cescatti, M. Dossena, P. del Giorgio, J.N. Gasol, J.M. Montoya, J. Pumpanen, P.A. Staehr, M. Trimmer, G. Woodward, and A.P. Allen. 2012. Reconciling the temperature dependence of respiration across timescales and ecosystem types. *Nature* 487: 472–476. https://doi.org/10.1038/nature11205.